Supporting Information

N-doped Fe$_2$(MoO$_4$)$_3$-decorated MoO$_3$ nanorods via metal-organic framework-involved synthesis as a bifunctional nanoreactor for capturing and catalyzing polysulfides in lithium-sulfur batteries

Zhi Hang Liu, Xiaoqing Mao, Xihao Liu, Yuanyan Luo, and Pei Kang Shen [*]

State Key Laboratory of Processing for Nonferrous Metals and Featured Materials; Guangxi Key Laboratory of Electrochemical Energy Materials; Collaborative Innovation Center of Sustainable Energy Materials, School of Physical Science and Technology, Guangxi University, Nanning 530004, China

*Corresponding authors: Prof. Pei Kang Shen (pkshen@gxu.edu.cn)

1. Experimental section

Materials Synthesis

In brief, 0.6 g of $(NH_4)_6Mo_7O_{24}·4H_2O$ and 2.5 mL of concentrated hydrochloric acid were added to 36 mL of deionized water. Then, the above solution was transferred to an autoclave and kept at 160 °C for 15 h. MoO_3 nanobelts were obtained after drying at 70 °C in the oven.

100 mg of the MoO_3 nanobelts, 1.12 g of $Fe_2SO_4·6H_2O$, and 2.4 g of polyvinylpyrrolidone were dispersed into 40 mL methanol to acquire solution A. 1.31 g of 2-methylimidazole was dissolved in 40 mL methanol to get solution B. Solution B was slowly dropped into solution A under magnetic stirring. After 2 h, the MoO_3/Fe-ZIF was collected by centrifugation and rinsed with ethanol. The $N-MoO_3@Fe_2(MoO_4)_3$ hybrid nanorods were gained by MoO_3/Fe-ZIF calcined at 500 °C for 2 h in a flow of air.

Materials Characterization

The morphology and structural characteristics of the fabricated samples were tested on Hitachi SU8220 scanning electron microscope (SEM) and Titan G2 transmission electron microscope (TEM) with energy dispersive X-Ray (EDX) spectroscopy. X-Ray Diffraction (XRD) results were recorded by a Rigaku D/Max-III diffractometer. Thermo Fisher Scientific ESCALAB 250XI+ photoelectron spectrometer with the Al Kα as the radiation source was used for XPS.

Preparation of coin cells and electrochemical measurement

To prepare a pure sulfur cathode, we used the standard sulfur cathode synthesis process: Ketjen black (KB) and sulfur were mixed with the polyvinylidene fluoride (PVDF) (mass ratio of 2:7:1) before adding moderate methyl-2-pyrrolidinone (NMP) for a slurry. The slurry was

coated onto an aluminum foil and dried immediately. The sulfur loading was about 1.2 mg cm^{-2}. The coating slurry is made by N-MoO$_3$@Fe$_2$(MoO$_4$)$_3$, KB, and PVDF (mass ratio of 7:2:1). The coated substrate is Cegard 2500 separator and the thickness is about 25 μm. The diameter of the cut circular separator was 18 mm. The thickness of the coating is about 10 μm, and the loading of such coating is about 0.20 mg cm^{-2}. Coin cells (CR2032) with a KB/S cathode (diameter of 14 mm), the functional separator (N-MoO$_3$@Fe$_2$(MoO$_4$)$_3$/PP), the lithium pieces anode, and the electrolyte (1 M LiTFSI in DOL/DME (volume ratio of 1:1) with 2 wt% LiNO$_3$) were assembled in an argon-filled glovebox. The galvanostatic charge-discharge measurements were tested on a Neware CT-4008T battery test system. The CV and EIS measurements were acquired on a Donghua DH7000 electrochemical workstation. The voltage window of the CV tests was 1.7-2.8 V and the frequency range of EIS tests was 0.01 Hz to 100 kHz.

Adsorption Test of LiPSs

To prepare 0.2 M Li$_2$S$_6$ solution, sulfur powder and Li$_2$S (molar ratio of 5:1) were added to the DOL/DME solution. After stirring at 50 °C for 12 h, 10 mg of N-MoO$_3$@Fe$_2$(MoO$_4$)$_3$, was added separately into glass bottles containing 0.15 mL of Li$_2$S$_6$ solution diluted in another 3.0 mL of DOL/DME solution. After 9 hours, the difference in color can be identified by eye observation. The adsorption capacity of N-MoO$_3$@Fe$_2$(MoO$_4$)$_3$ was further confirmed via UV-vis spectra tested by HORIBA FluoroMax-4 fluorescence spectrometer.

Permeation Tests of Li$_2$S$_6$

N-MoO$_3$@Fe$_2$(MoO$_4$)$_3$/PP was used to separate the H-type glass electrolysis cells. 0.01 M prepared Li$_2$S$_6$ solution is on the left, and the Li$_2$S$_6$-free DOL/DME solution was on the other side. The color change was recorded after 6 hours to compare the permeation of LiPSs.

Assembly of Symmetric Cells and Tests

Sample (N-MoO$_3$@Fe$_2$(MoO$_4$)$_3$ or MoO$_3$), carbon black, and PVDF (mass ratio 7:2:1) were mixed in NMP to prepare a uniform slurry. The slurry was then evenly coated on carbon paper and dried immediately. After that, the carbon paper was punched into several disks (diameter: 14 mm, load: 2 mg) as the working electrodes and counter electrodes. The electrodes were assembled into a CR2032 coin cell with 60 μL of DOL/DME electrolyte containing Li$_2$S$_6$ (0.1 M) and LITFSI (1M). CV curves were carried out to access the performance of symmetric cells. The scan velocity was 50 mV s^{-1} between -1 V to 1 V.
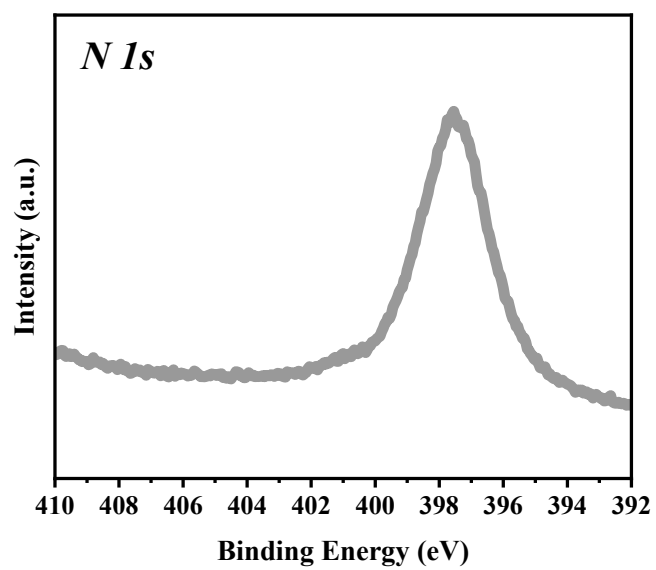
2. Supporting Figures
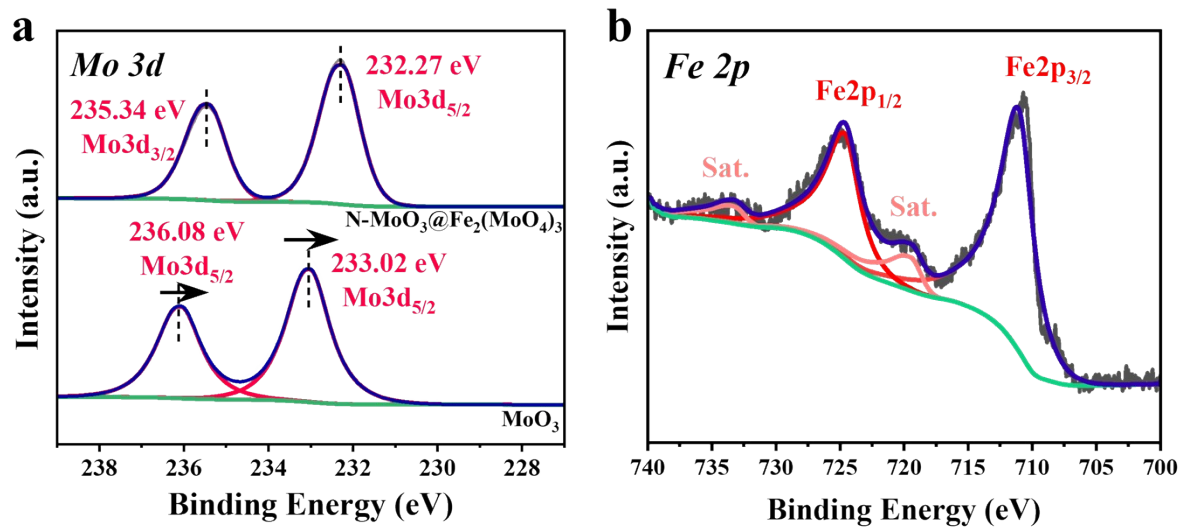

Fig. S1. High-resolution XPS spectrum of N 1s

Fig. S2. High-resolution XPS spectra of (a) Mo 3d of N-MoO$_3$@Fe$_2$(MoO$_4$)$_3$ and MoO$_3$ and (b) Fe 2p of MoO$_3$.
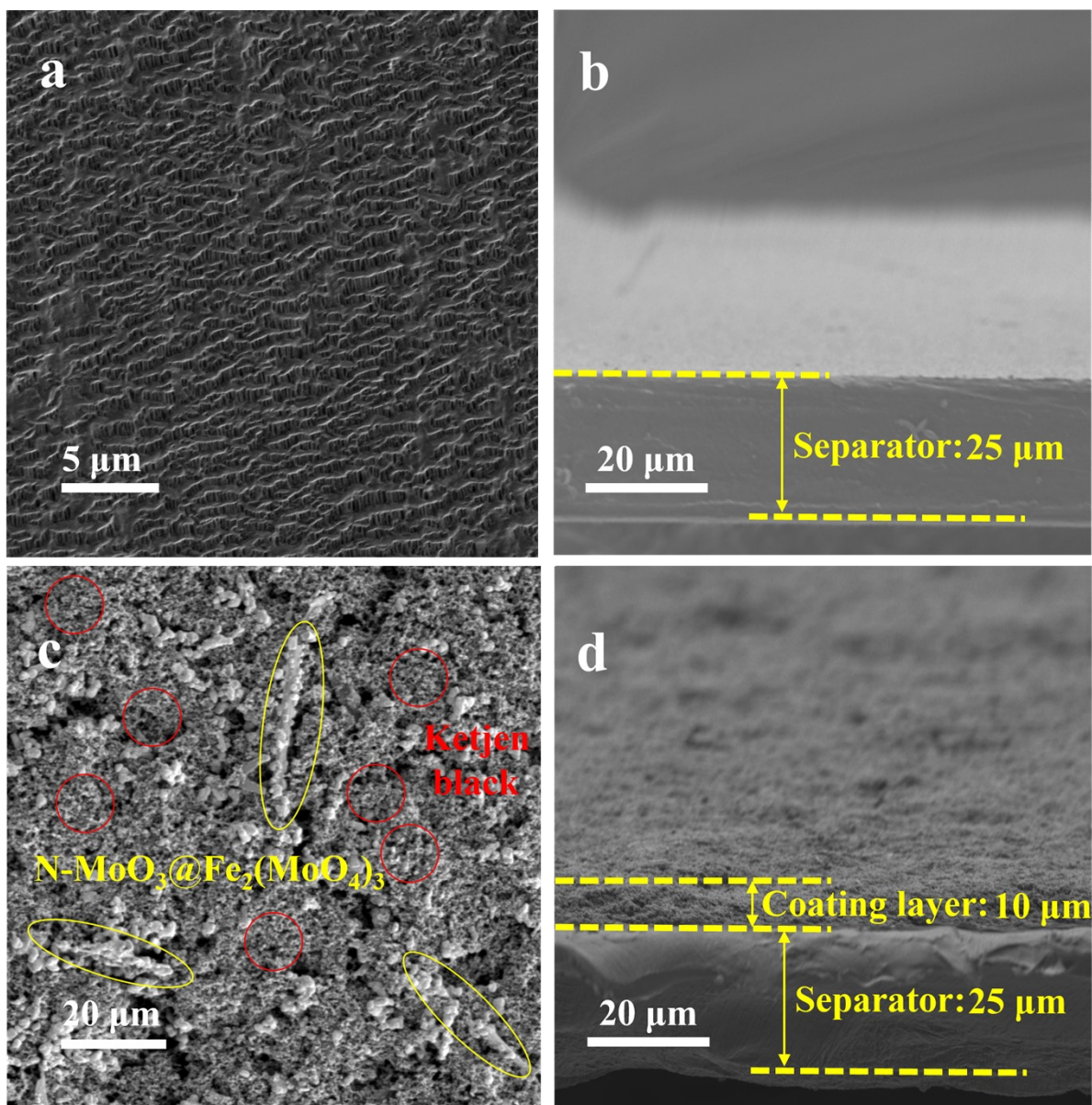
Fig. S3. Horizontal plane (a, c) and cross-sectional (b, d) SEM images of the N-MoO$_3$@Fe$_2$(MoO$_4$)$_3$/PP and PP separator.

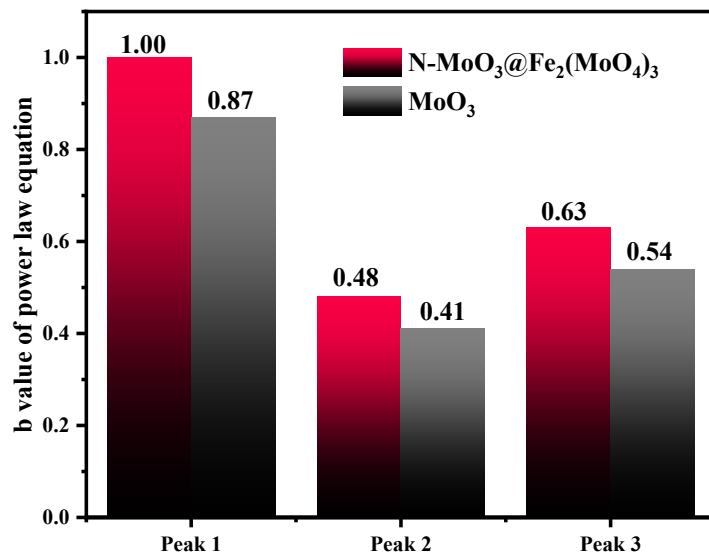**Fig. S4.** Li_2S_6 permeation experiment of H-shaped glass tubes with MoO_3/PP.
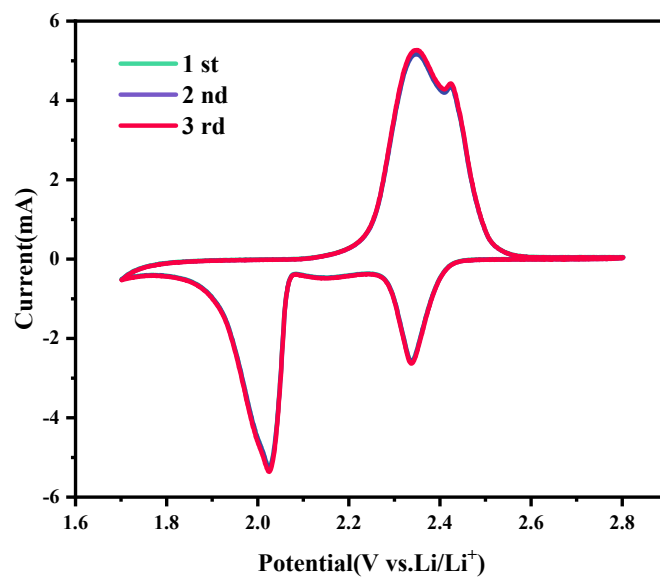
Fig. S5. B value of the power-law equation in peak1-3.

Fig. S6. The first three cycles of CV curves of cells with N-MoO$_3$@Fe$_2$(MoO$_4$)$_3$/PP.
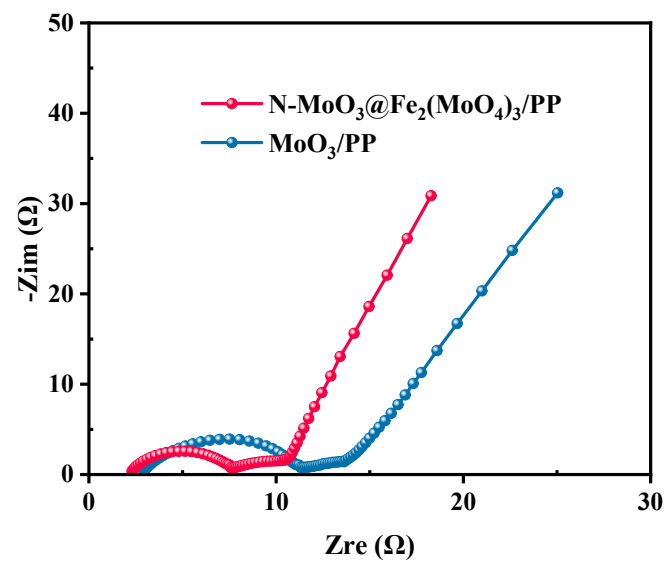
Fig. S7. EIS spectra of cells with different separators after 0.5C for 100 cycles.

Table S1. Comparison of the electrochemical performance of N-MoO$_3$@Fe$_2$(MoO$_4$)$_3$ with other reported separator coating materials.

Cathode	sulfur loading (mg cm^{-2})	Coating material	Initial capacity (mAh g^{-1})	Capacity fading rate (per cycle)	year	Refs
Pure sulfur	1.2	N-MoO$_3$@Fe$_2$(MoO$_4$)$_3$	1601 (0.1C)	0.05% (600r-1C)	2022	This work
Pure sulfur	0.8-1.0	Zn, N-doped carbon nanofiber	1263 (0.2C)	0.07%(500r-1C)	2022	[1]
Pure sulfur	0.7	TiN@C	1490 (0.1C)	0.05% (600r-1C)	2021	[2]
Pure sulfur	1.2-1.4	Li-MOF/RGO	~1600 (0.1C)	0.09% (600r-1C)	2021	[3]
Pure sulfur	1.1-1.4	P-CoS$_2$/CNT	1643 (0.1C)	0.06% (500r-1C)	2021	[4]
Sulfur composite	1.0-1.2	Ni/SiO$_2$/G	1456 (0.1C)	0.09% (300r-1C)	2020	[5]
Pure sulfur	1.2	NiS$_2$@rGO/CNTs-Li	1515 (0.2C)	0.07% (600r-2C)	2020	[6]
Sulfur composite	1.2	Oxi-d-Mxene900	~1600 (0.2C)	0.14% (300r-1C)	2020	[7]
Pure sulfur	1.0	P-doped BN/graphene	~1500 (0.1C)	0.06% (500r-1C)	2019	[8]
Pure sulfur	1.2	PPy	1271 (0.1C)	0.08% (250r-0.5C)	2019	[9]
Pure sulfur	1.0	ZBCP	1407 (0.1C)	0.05% (200r-0.25C)	2018	[10]
Pure sulfur	1.2	MoS$_2$/Polymer	~1450 (0.1C)	0.05% (600r-1C)	2018	[11]

Supplementary References

1. X. Fang, P. Cheng, K. Sun, Y. Fu, D. Liu and D. He, *ACS Applied Energy Materials*, 2022, **5**, 8189-8197.

2. Y. Fan, K. Liu, A. Ali, X. Chen and P. K. Shen, *Electrochim Acta*, 2021, **384**.

3. M. Zhou, Y. Li, T. Lei, W. Chen, G. Rao, L. Xue, A. Hu, Y. Fan, J. Huang, Y. Hu, X. Wang and J. Xiong, *Small*, 2021, **17**, e2104367.

4. J. Liu, Z. Qiao, Q. Xie, D. L. Peng and R. J. Xie, *ACS Appl Mater Interfaces*, 2021, **13**, 15226-15236.

5. C. Chen, Q. B. Jiang, H. F. Xu, Y. P. Zhang, B. K. Zhang, Z. Y. Zhang, Z. Lin and S. Q. Zhang, *Nano Energy*, 2020, **76**.

6. J. Wang, J. Xu, W. Q. Tang, D. F. Niu, S. L. Zhao, S. Z. Hu and X. S. Zhang, *Chemnanomat*, 2020, **6**, 976-983.

7. D. K. Lee, Y. Chae, H. Yun, C. W. Ahn and J. W. Lee, *ACS Nano*, 2020, **14**, 9744-9754.

8. J. Zhang, W. Ma, Z. Feng, F. Wu, D. Wei, B. Xi and S. Xiong, *Journal of Energy Chemistry*, 2019, **39**, 54-60.

9. Y. J. Li, W. Y. Wang, X. X. Liu, E. Y. Mao, M. T. Wang, G. C. Li, L. Fu, Z. Li, A. Y. S. Eng, Z. W. Seh and Y. M. Sun, *Energy Stor Mater*, 2019, **23**, 261-268.

10. J. K. Huang, M. Li, Y. Wan, S. Dey, M. Ostwal, D. Zhang, C. W. Yang, C. J. Su, U. S. Jeng, J. Ming, A. Amassian, Z. Lai, Y. Han, S. Li and L. J. Li, *ACS Nano*, 2018, **12**, 836-843.

11. J. Y. Wu, H. X. Zeng, X. W. Li, X. Xiang, Y. G. Liao, Z. G. Xue, Y. S. Ye and X. L. Xie, *Adv Energy Mater*, 2018, **8**.